◆ Human Brain Mapping 36:3912–3921 (2015) ◆

The Influence of Mild Carbon Dioxide on Brain Functional Homotopy Using resting-State fMRI

Olga Marshall,[1] Jinsoo Uh,[2] Daniel Lurie,[3] Hanzhang Lu,[2,4] Michael P. Milham,[3,5] and Yulin Ge[1]*

[1]*Radiology/Center for Biomedical Imaging, New York University School of Medicine, New York, New York*
[2]*Advanced Imaging Research Center, University of Texas Southwestern Medical Center, Dallas, Texas*
[3]*Center for the Developing Brain, Child Mind Institute, New York, New York*
[4]*Department of Radiology, Johns Hopkins University School of Medicine, Baltimore, Maryland*
[5]*Nathan S Kline Institute for Psychiatric Research, New York*

Abstract: Homotopy reflects the intrinsic functional architecture of the brain through synchronized spontaneous activity between corresponding bilateral regions, measured as voxel mirrored homotopic connectivity (VMHC). Hypercapnia is known to have clear impact on brain hemodynamics through vasodilation, but have unclear effect on neuronal activity. This study investigates the effect of hypercapnia on brain homotopy, achieved by breathing 5% carbon dioxide (CO_2) gas mixture. A total of 14 healthy volunteers completed three resting state functional MRI (RS-fMRI) scans, the first and third under normocapnia and the second under hypercapnia. VMHC measures were calculated as the correlation between the BOLD signal of each voxel and its counterpart in the opposite hemisphere. Group analysis was performed between the hypercapnic and normocapnic VMHC maps. VMHC showed a diffused decrease in response to hypercapnia. Significant regional decreases in VMHC were observed in all anatomical lobes, except for the occipital lobe, in the following functional hierarchical subdivisions: the primary sensory-motor, unimodal, heteromodal, paralimbic, as well as in the following functional networks: ventral attention, somatomotor, default frontoparietal, and dorsal attention. Our observation that brain homotopy in RS-fMRI is affected by arterial CO_2 levels suggests that caution should be used when comparing RS-fMRI data between healthy controls and patients with pulmonary diseases and unusual respiratory patterns such as sleep apnea or chronic obstructive pulmonary disease. *Hum Brain Mapp 36:3912–3921, 2015.*

Key words: resting-state; functional MRI; hypercapnia; brain; connectivity; homotopy

Contract grant sponsor: National Institute of Health of R01; Contract grant numbers: NS029029S1, NS076588, MH084021, NS067015, and AG042753; Contract grant sponsor: National Multiple Sclerosis Society research grant; Contract grant number: RG4707A.

*Correspondence to: Yulin Ge; Department of Radiology, Center for Biomedical Imaging, New York University School of Medicine, 660 First Avenue, 4th floor, New York, NY 10016. E-mail: yulin.ge@nyumc.org

Received for publication 4 February 2015; Revised 9 June 2015; Accepted 16 June 2015.

DOI: 10.1002/hbm.22886

Published online 2 July 2015 in Wiley Online Library (wileyonlinelibrary.com).

INTRODUCTION

Homotopy is a fundamental feature of the intrinsic functional architecture of the human brain by describing the interhemispheric symmetry and synchrony. In the resting brain, not only is there highly synchronous activity in immediately neighboring areas, but also between corresponding regions in the left and right hemisphere, which are geometrically and often functionally corresponding to each other. This is essential for dynamic interhemispheric communication and coordination for lower-order neurological processes, such as sensory inputs and motor outputs that require the automatic integration of information [Fair et al., 2007]. Conversely, two sides of the brain differ in certain specialized functions and roles, as higher order systems that involve complex attention and cognitive processes are mostly lateralized [Zou et al., 2008] and do not require highly synchronized activity between the two hemispheres. This brain lateralization, or dominance, is thought to be developed during childhood [Zuo et al., 2010b] and several studies have shown asymmetric cerebral blood flow (CBF) during picture description, word generation, or visuospatial tasks (i.e., high order cognitive tasks) measured with functional magnetic resonance imaging (fMRI) [Benson et al., 1999] or functional transcranial Doppler ultrasound [Bulla-Hellwig et al., 1996; Rihs et al., 1995; Schmidt et al., 1999]. These data may support the theory that functional specialization of one hemisphere may be related to the underlying development of asymmetric human cerebral circulation as a result of adaptive dynamic blood flow response to dominant functional activity from one side of brain [Aaslid, 1987].

Recently, the degree of interhemispheric synchrony or homotopy has been estimated with blood oxygenation level dependent (BOLD) spontaneous activity during resting state fMRI (RS-fMRI) scans [Stark et al., 2008], using the voxel mirrored homotopic connectivity (VMHC) measure, which quantifies the functional connectivity strength between each voxel and its mirrored counterpart in the opposite hemisphere. It has been suggested [Stark et al., 2008] that the strength of VMHC may be related to the extent of regional functional specialization. Previous studies [Zuo et al., 2010b] have found strong developmental and age-related changes of VMHC predominantly in areas supporting higher-order cognitive processes. The regional differences which reflect the various degrees of lateralization of function in the human brain correspond with the region's various developmental trajectories of homotopic connectivity, strongly resembling the maturation pattern of these structures [Zuo et al., 2010b]. VMHC has been used to study the interhemispheric disturbance of functional coordination [Wise et al., 2004; Zuo et al., 2010b] in several neurological diseases [Kelly et al., 2011; Zhou et al., 2013].

Carbon dioxide (CO_2) is a potent vasodilator which has been known to cause CBF and BOLD signal changes, and hypercapnia magnetic resonance imaging (MRI) has been emerged as a new tool to estimate brain vascular health [Lu et al., 2011, 2014; Marshall et al., 2014; Yezhuvath et al., 2009]. The effect of mild hypercapnia (5% CO_2) was originally thought to affect the vasculature alone without altering neuronal activity [Kety and Schmidt, 1948]. Even though recent studies have shown a decrease in metabolic activity, by cerebral metabolic rate of oxygen ($CMRO_2$) measurements, and a decrease in spontaneous activity in the brain due to CO_2 induced hypercapnia [Xu et al., 2011; Yuan et al., 2013], a debate still exists surrounding the precise effect of hypercapnia on metabolic activity [Chen and Pike, 2010; Jain et al., 2011; Mark et al., 2011; Sicard and Duong, 2005; Yablonskiy, 2011; Zappe et al., 2008]. The exact mechanism of vascular and neuronal involvement causing the hypercapnia related changes is still poorly understood. Previous studies have also indicated that small fluctuations in end-tidal CO_2 ($EtCO_2$) occur during normal breathing, due to changes in the depth and rate of breaths, which are correlated with fluctuations in the BOLD signal [Birn et al., 2006; Wise et al., 2004], and may potentially influence RS-fMRI data analysis. Therefore, a thorough understanding and characterization of these changes are essential to better understand and compensate for their effect due to naturally occurring physiological respiratory (e.g., CO_2 changes) and cardiac (e.g., flow changes) noise in BOLD and RS-fMRI studies. Although there are a few studies [Biswal et al., 1997; Xu et al., 2011] on CO_2 effects on functional connectivity, to date, no study has inspected the CO_2 effects on brain functional homotopic connectivity with RS-fMRI.

The goal of the current study is to investigate the mild hypercapnia effects on brain homotopy by measuring voxel based VMHC changes as a result of well controlled variation in arterial CO_2 levels monitored by $EtCO_2$ during RS-fMRI scans. We will also demonstrate the homotopic alterations of intrinsic interhemispheric networks that may respond differently to elevated blood CO_2 levels.

MATERIALS AND METHODS

Participants

Fourteen healthy controls (8 male and 6 female, 27.6 ± 6.4 years old) participated in this study after providing written consent. This protocol was approved by the Institutional Review Board of the University of Texas Southwestern Medical Center. Participants had no history of neurological or psychiatric disease.

MRI Imaging

MRI data was acquired on a 3 Tesla MRI scanner (Philips Medical System, Best, The Netherlands). RS-fMRI sequences were acquired with the following imaging parameters: TR/TE=1,500/25 ms, FOV = 220 × 220 mm^2, matrix = 64 × 64, number of slices = 33, slice thickness = 3 mm, 200 measurements, total scan time = 5 min. Three

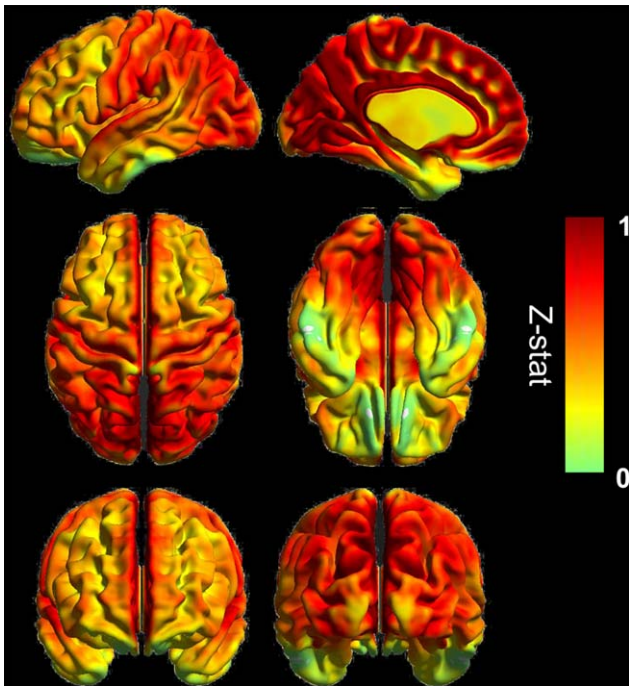

Figure 1.

Averaged VMHC map at normocapnia ($N = 14$), with the color bars showing the z-statistics of the measure. Surface rendering in left lateral and mid-sagittal (top row), dorsal and ventral (middle row), anterior and posterior (bottom row) views visualized by BrainNet Viewer (http://www.nitrc.org/bnv). [Color figure can be viewed in the online issue, which is available at wileyonlinelibrary.com.]

such scans were completed, the first and third under a normocapnia condition (breathing room air) and the second under a hypercapnia condition (breathing a mixture of 5% CO_2, 21% O_2, and 72% N_2). Every time a change was made in the breathing paradigm and the gas delivered to the patient was switched (between room air and the 5% CO_2 mixture) a short 2 min time delay was implemented to account for the time needed for the gas to reach the mouthpiece through the breathing apparatus and for $EtCO_2$ levels to stabilize. This time also allows for arterial arrival time to the brain, which usually occurs within 15 s, and BOLD signal stabilization, which occurs instantaneously with vascular changes. [Xu et al., 2011; Yezhuvath et al., 2009]. The $EtCO_2$ is a measurement, which quantifying the CO_2 content in the lungs, is typically at equilibrium with the arterial CO_2 partial pressure [Ibler et al., 1992]. It was ensured that this level reached steady state before scans were started, which was monitored and recorded throughout the experiment on a capnograph device (Capnogard, Model 1265, Novametrix Medical Systems, CT). The air was manipulated by a previously described gas delivery system [Xu et al., 2011]. Subjects were introduced to the breathing apparatus prior to the scan, therefore, minimizing subject motion during the scan due to unfamiliarity with the setup. Additionally, changes in the delivered gas (whether room air or the 5% CO_2 mixture) could be made without stopping the scan or moving the subject, which also decreased the length of the study and discomfort for the patient.

In addition to functional scans, a high resolution anatomical T1-weighted image, with the following parameters: shot interval 2,100 ms, TR/TE/TI = 8.2/3.8/1,100 ms, voxel size = 1 mm isotropic was acquired for image coregistration and segmentation.

Image Processing

RS-fMRI data were processed using the Configurable Pipeline for the Analysis of Connectomes (http://fcp-indi.github.com/C-PAC/) to generate the VMHC [Zuo et al., 2010b] metric. Preprocessing steps included slice-timing and motion correction (using the Friston 24-Parameter Model [Friston et al., 1996]), nuisance signal regression (including 6 motion parameters, CompCor signals [Ziyeh et al., 2005], and linear and quadratic trend), and temporal filtering of signal between 0.01 and 0.1 Hz [Gee et al., 2011; Schroeder and Lakatos, 2009; Zuo et al., 2010a]. As subjects completed these scans while wearing the mouthpiece, quality control was performed with extra attention so that subjects with excessive motion or problems with the mouthpiece or nose clip were excluded.

VMHC maps were generated by calculating the correlation between each voxel and its counterpart on the opposite hemisphere after registration to a symmetric template brain [Zuo et al., 2010b]. After normalization to Montreal Neurological Institute (MNI) 152 space, the correlation coefficient at each voxel was Fisher z-transformed. For group analysis, spatial smoothing using a 6 mm full-width half-maximum Gaussian kernel was completed. The average normocapnic voxel based VMHC map generated can be seen in Figure 1 as a surface rendering.

Regional analysis was completed by taking the average VMHC measure across all voxels within regions defined by the MNI structural atlas (frontal, parietal, temporal, and occipital lobes, deep gray matter structures, the cerebellum, as well as the entire gray matter (GM), calculated based on the standard GM map within the previously listed regions), functional hierarchical subdivisions as described in Mesulam [1998] (primary sensory-motor cortices, unimodal association areas, heteromodal association areas, paralimbic, limbic, and subcortical areas) and functional networks as described by Yeo et al. [2011] (visual, somatomotor, dorsal attention, ventral attention, limbic, frontoparietal, and default). As the definition of the limbic regions is not consistent, we refer to two different classification schemes to describe the limbic network. In the hierarchical classification, the hippocampus and amygdala are included; in the functional classification only the cortical areas which represent the functionally coupled regions of the limbic network are included.

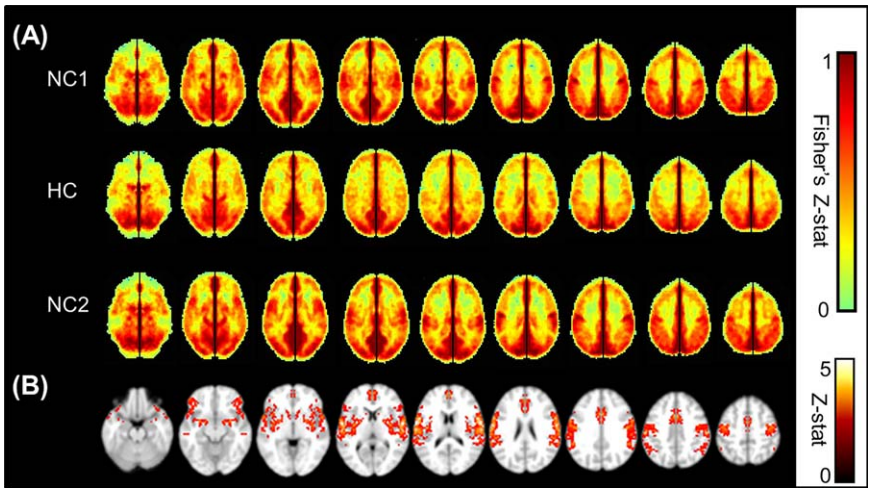

Figure 2.

(**A**) Average VMHC maps showing Fisher Z-transformed correlation, restricted to GM only, of the first normocapnic run (NC1), the hypercapnic run (HC), and the second normocapnic run (NC2). Enough time (at least 2 min) was given each time the delivered air was switched between normocapnia and hypercapnia, to allow end tidal CO_2 to return to a steady state. A global decrease in VMHC is seen under hypercapnia, which is restored to the original magnitude in the final normocapnia run. The color bar shows the limits of the *Z*-score values. (**B**) Significant group decrease from NC1 to HC shown as a result of a voxel by voxel pairwise comparison of the Fisher's Z-transformed VMHC maps, performed in FSL/FEAT (minimum $Z > 2.3$; cluster level, $P < 0.05$, corrected). [Color figure can be viewed in the online issue, which is available at wileyonlinelibrary.com.]

Statistical Analysis

Average regional values of the first normocapnic (NC1) and second normocapnic (NC2) scan and the hypercapnic (HC) scan were compared using a paired Student's *t*-test. False discovery rate correction was applied to correct for multiple comparisons.

Differences in the VMHC maps under the various conditions were analyzed using a voxel by voxel pairwise comparison performed with a General Linear Model based comparison using FSL/FEAT functions (FMRIB's Software Library, http://www.fmrib.ox.ac.uk/fsl) as built into the C-PAC processing stream. Multiple comparison correction was performed based on Gaussian random field theory (minimum $Z > 2.3$, cluster level $P < 0.05$ corrected).

RESULTS

The average (±SD) $EtCO_2$ increased significantly from the NC1 to the HC condition (40.15 ± 2.63 to 47.39 ± 2.74 mm Hg, NC1 vs. HC and NC2 vs. HC $P < 0.01$) and returned to the baseline level or lower for the NC2 scan (38.68 ± 3.07 mm Hg, NC1 vs. NC2 $P < 0.01$). The breathing rate and heart rate did not change significantly during any of the three resting state scans. The average breathing rate (breaths/min) during the NC1 and NC2 scans were 13.4 ± 3.5 and 13.4 ± 2.9, respectively, and during the hypercapnia scan was 11.0 ± 4.9 (NC1 vs. HC, $P = 0.2$). The average heart rate (beats/min) during the NC1 and NC2 scan were 64.4 ± 14.4 and 56.8 ± 14.6, respectively, and during the HC scan was 67.0 ± 15.9 (NC1 vs. HC, $P = 0.08$).

Visual inspection of the average maps (Fig. 2a) shows a diffuse decrease in VMHC under HC compared with the NC1 and NC2 conditions. The VMHC amplitude returns to baseline in the NC2 condition, indicating that the effects of hypercapnia are transient. The result of the voxel-by-voxel comparison of the NC1 and HC VMHC maps can be seen in Figure 2b. Only voxels that show a significant decrease due to hypercapnia are displayed (corrected $P < 0.05$).

Average values of VMHC classified by anatomical regions, functional hierarchy, and functional networks are listed in Table I, with the *P* value showing the result of a paired *t*-test corrected for multiple comparisons between the values of the NC1 and the HC scan. A significant decrease in VMHC is seen in all anatomical areas except for the occipital lobe. There is a significant decrease in global GM VMHC under HC versus the NC1 (0.41 ± 0.06, 0.33 ± 0.09, $P < 0.001$), which returns to the baseline level during the NC2 (0.42 ± 0.06). Global GM VMHC values are stable between the two normocapnic runs ($P = 0.4$), and so were all other anatomical regions. The percent decrease in the averaged VMHC values from NC1 to HC is between 14 and 20% across regions which are statistically significant, but the extent of reduction is only about 3% in the occipital lobe. Twelve percent of the whole brain GM voxels was found to show a significant decrease

TABLE I. Regional comparison of average VMHC between the first normocapnia (NC1) and hypercapnia

Region		NC1	HC	*P* value NC1 versus HC	% of significantly decreased in each region
Anatomical subdivisions	Deep GM	0.47 ± 0.08	0.38 ± 0.09	0.006*	19.80%
	Frontal lobe	0.50 ± 0.09	0.40 ± 0.11	0.0007*	14.74%
	Parietal lobe	0.67 ± 0.13	0.58 ± 0.15	0.001*	13.28%
	Whole brain GM	0.56 ± 0.08	0.48 ± 0.10	0.002*	12.00%
	temporal lobe	0.39 ± 0.06	0.32 ± 0.09	0.0003*	7.41%
	Occipital lobe	0.75 ± 0.12	0.73 ± 0.15	0.3	0%
Functional network subdivisions	Ventral attention	0.52 ± 0.11	0.38 ± 0.12	<0.0001*	33.70%
	Somatomotor	0.61 ± 0.19	0.45 ± 0.21	<0.0001*	33.39%
	Default	0.56 ± 0.07	0.47 ± 0.11	0.002*	9.27%
	Frontoparietal	0.46 ± 0.10	0.38 ± 0.10	0.007*	4.58%
	Dorsal attention	0.57 ± 0.14	0.51 ± 0.15	0.03*	4.01%
	Limbic	0.25 ± 0.06	0.22 ± 0.09	0.05	1.62%
	Visual	0.7 ± 0.11	0.67 ± 0.13	0.2	0%
Functional hierarchical subdivisions	Primary SM	0.68 ± 0.14	0.54 ± 0.16	0.0001*	33.97%
	Paralimbic	0.49 ± 0.06	0.39 ± 0.08	<0.0001*	18.14%
	Unimodal	0.60 ± 0.09	0.51 ± 0.13	0.001*	12.56%
	Subcortical	0.57 ± 0.09	0.52 ± 0.08	0.1	10.24%
	Heteromodal	0.56 ± 0.09	0.46 ± 0.12	0.002*	9.13%
	Limbic	0.45 ± 0.08	0.40 ± 0.06	0.1	7.20%

Note: Average voxel based VMHC values within the listed regions were compared between the fist normocapnic (NC1) and the HC scan using a paired *t*-test (FDR corrected $P < 0.05$). Statistically significant comparisons are marked by *. Comparing the first and second normocapnic scans, no regions showed a significant difference in VMHC. Additionally, the percent of each region is indicated, which shows a significant decrease as a result of the voxel based group analysis (corrected $P < 0.05$ considered significant).

in VMHC as revealed by the voxel-wise group analysis. Dividing them by regions, about 20% of the deep GM structures, more than 10% of the frontal and parietal lobes, about 8% of the temporal lobe, and none of the occipital lobe voxels was found to show a significant effect (Table I).

Similarly, average VMHC values within the functional networks are listed (Table I) as well as displayed (Fig. 3). The visual network is the only network which did not show a significantly decreased VMHC value in response to hypercapnia. The limbic network showed a significant decrease during HC only when compared with NC2 ($P = 0.002$), but not compared with NC1 and was the only network to have a significant difference between the two normocapnic VMHC values ($P = 0.03$). The dorsal attention, frontoparietal, and default networks showed a significant decrease of the NC1 VMHC value in response to hypercapnia (corrected $P < 0.05$) and none of these networks showed a significant change when comparing the HC or NC1 values to the NC2 values. The percent decrease in VMHC measure from NC1 to HC is greater than 20% in the ventral attention and somatomotor networks, which also had the greatest percentage of the region significant in the voxel based analysis (>30% of GM). Furthermore, the default, frontoparietal, dorsal attention, and limbic networks had a greater than 10% VMHC decrease due to hypercapnia, but under 10% of the network's areas was significant in the voxel based group analysis (Table I).

Within the functional hierarchical subdivisions, average VMHC values are listed (Table I) as well as displayed (Fig. 4). The primary sensory-motor, unimodal, heteromodal, and paralimbic subdivisions show significantly decreased VMHC under the HC condition when compared with both NC1 and NC2 (corrected $P < 0.05$). The limbic and subcortical subdivisions only show significantly decreased VMHC under HC when compared with NC2, not to NC1 (corrected $P < 0.05$). None of the subdivisions show a significant difference between the average NC1 and NC2 values. The percent decrease in VMHC measure from NC1 to HC is about 20% in the primary somatomotor and paralimbic regions, greater than 10% in the unimodal and heteromodal regions, and less than 10% in the subcortical and limbic regions. About 34% of the primary somato-motor regions's area was found significant using voxel based group analysis, but only greater than 10% of the paralimbic, unimodal, and subcortical regions, and just under 10% of the heteromodal and limbic regions (Table I).

DISCUSSION

Although RS-fMRI has rapidly emerged as a powerful noninvasive technique for studying brain functional networks, few studies have investigated the hemodynamic and physiologic basis of function connectivity between given homologous brain regions. The underlying mechanism of the BOLD signal is still debated, but CBF studies

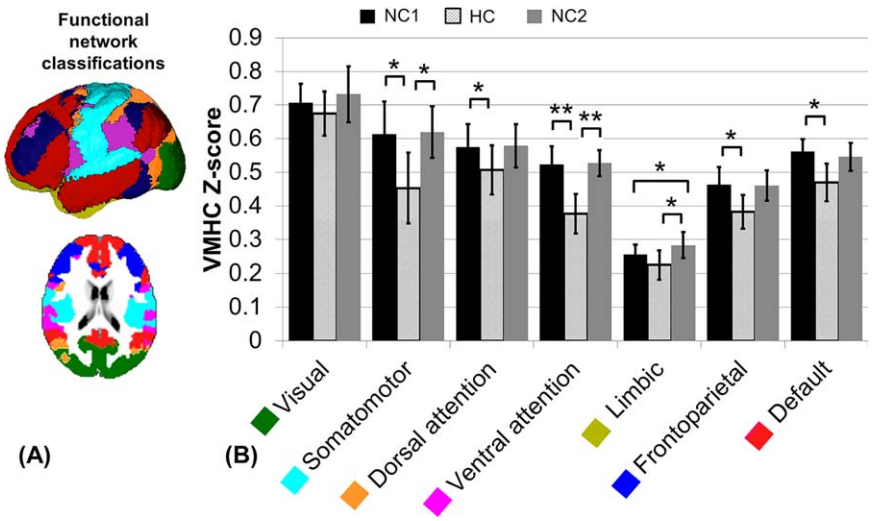

Figure 3.

(**A**) Functional network classification as described by Yeo et al [2011]: visual (green), somatomotor (light blue), dorsal attention (yellow), ventral attention (magenta), limbic (gold), frontoparietal (dark blue), and default (red). (**B**) Comparison of average VMHC Fisher Z-transformed values during the first normocapnic (NC1), HC and second normocapnic (NC2) scans, calculated as the average of the voxel based map within each region. Error bars show standard deviation. Significance calculated based on a paired *t*-test between each normocapnic and the HC scan (FDR corrected $P < 0.05$). There was no significant difference between the NC1 and NC2 values, except for the limbic network ($P = 0.03$). *$P < 0.05$, **$P < 0.01$, ***$P < 0.001$. [Color figure can be viewed in the online issue, which is available at wileyonlinelibrary.com.]

of neurovascular coupling suggest that there is physiological significance of the RS-fMRI measures [Mark et al., 2015]. Our results demonstrate that there is a varied degree of decreased brain homotopy during mild hypercapnia and such decrease is recovered shortly after these subjects return to breathing room air. RS-fMRI connectivity analysis is based on blood flow mediated BOLD signal fluctuations. This allows connectivity measures to be

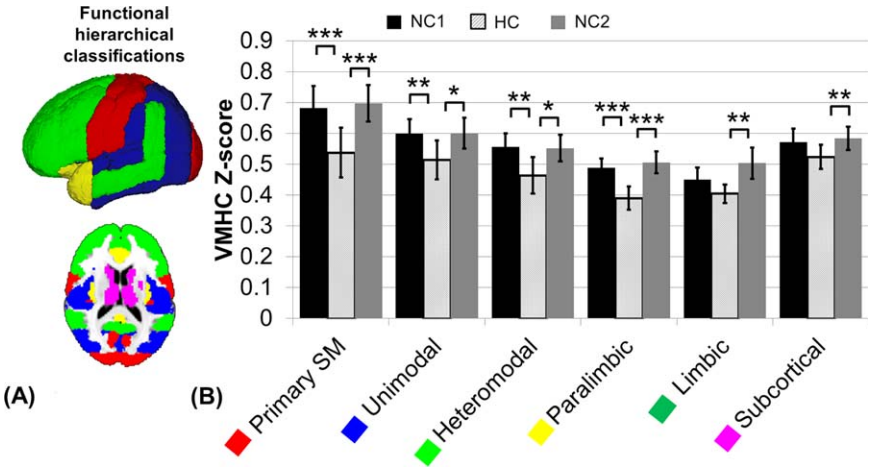

Figure 4.

(**A**) Functional hierarchical classification as identified by Mesulam [1998]: primary somato-motor (red), unimodal (blue), heteromodal (light green), paralimbic (yellow), limbic (green, not shown in figure), and subcortical (magenta). (**B**) Comparison of average VMHC Fisher Z-transformed values during the first normocapnic (NC1), HC and second normocapnic (NC2) scans, calculated as the average of the voxel based map within each region. Error bars show standard deviation. Significance calculated based on a paired *t*-test between each normocapnic and the HC scan (FDR corrected $P < 0.05$). There was no significant difference between the NC1 and NC2 values. *$P < 0.05$, **$P < 0.01$, ***$P < 0.001$. [Color figure can be viewed in the online issue, which is available at wileyonlinelibrary.com.]

impacted by the CO_2 challenge, which is known to cause significant increase in CBF [Kim et al., 1999] during mild hypercapnia (5% CO_2 mixture). Studies seeking to determine these effects will help better interpret RS-fMRI data and show the importance of BOLD signal variation in subjects with irregular breathing patterns such as breath hold [Biswal et al., 2007] or in patients with comorbid condition from various respiratory diseases.

Our results are consistent with previous reports, albeit few [Biswal et al., 1997; Xu et al., 2011], in which elevated arterial CO_2 is shown to decrease brain functional connectivity. Early work by Biswal et al. [1997] showed a substantial increase of magnitude of the BOLD signal at the higher physiological frequency (i.e., >0.1 Hz), but a decrease at lower frequencies (<0.08 Hz) across all subjects and motor cortex voxels, suggesting mild CO_2 can reversibly suppresses low-frequency fluctuations. A recent study by Xu et al. [2011] found that hypercapnia reduced functional connectivity measurements including network cluster volume, cross-correlation coefficient, and amplitude of the functional connectivity MRI signal in the default-mode network, which is a commonly described resting state network. The exact mechanism of such changes is still not fully understood, but may relate to the mixed hypercapnia effect on both blood flow (i.e., oxygen supply) and neural activity. Previous studies performed at 3T showed that CO_2, a vasodilator, can cause about 40–55% increase in CBF [Kim et al., 1999; Xu et al., 2011] about 13% decrease in metabolic rate [Xu et al., 2011], as measured by $CMRO_2$, and about 3% BOLD signal intensity increases [Yezhuvath et al., 2009]. Also, there is evidence that CO_2 has a dose dependent effect on $CMRO_2$, showing a correlation between neuronal activity decrease and arterial CO_2 level increase [Xu et al., 2011]. These factors have the potential to alter the level of interhemispheric synchronous activity, which we currently estimate by VMHC.

VMHC is a voxel-based method which estimates the degree of synchrony between geometrically corresponding interhemispheric mirrored voxels by evaluation of the strength of their functional connectivity [Zuo et al., 2010b]. Although homotopy is an intrinsic and fundamental feature of brain's functional architecture, the strength of this interhemispheric functional synchrony varies across brain regions due to developmental lateralization from the learning process as well as learning ability. Consistent with previous literature [Stark et al., 2008], we also found strongest homotopy within visual, motor and somatosensory cortex and relatively weaker in prefrontal and temporoparietal association areas. These weaker regions are known for increased functional lateralization related to high-order cognitions such as language, attention, and memory [Jones-Gotman, 1986; Kimura and Archibald, 1974]. In RS-fMRI, BOLD signal fluctuations are associated with regional blood flow fluctuations together with the changes of blood oxygenation and baseline neuronal activity. One possible explanation for the spatially varied effect of hypercapnia on VMHC is that the bilateral and corresponding synchronous regions may have different microvascular networks that are formed asymmetrically during developmental lateralization. During various task-induced neural activities, previous studies have shown hemispheric asymmetry of arterial blood flow or flow velocity measured with fMRI [Benson et al., 1999] or transcranial Doppler sonography [Bulla-Hellwig et al., 1996; Haag et al., 2010; Schmidt et al., 1999]. Uneven changes in the neuronal activities which lead to asynchronous BOLD signal fluctuations may contribute to different amounts of arterial flow reaching homotopic areas. This reflects that areas will experience a larger amount of homotopic disruption due to increased arterial CO_2 levels if their underlying regional vascular distribution is more dominant on one side, as seen in the strong effect of hypercapnia on the ventral attention network. Similarly, the motor network shows a strong disruption in VMHC due to increased arterial CO_2 levels, which may be attributed to asymmetric blood flow due to dominant side of brain (i.e., handedness) [Gur et al., 1982].

Although the effects of increased arterial CO_2 will cause a global effect, it is difficult to have such fine control over individual arteries to ensure precisely the same amount of increased blood flow throughout the brain. Therefore, imbalanced blood delivery to corresponding bilateral regions may lead to imbalanced arterial CO_2 levels, causing a decrease in synchronous activity. Although the primary visual cortex has higher VMHC than areas such as the primary motor cortex, it behaves differently in that we did not observe significant changes during hypercapnia. This finding merits more research to identify the underlying causes of regional variation, but one suggestion is that it may be due to the vascular differences of the visual cortex, such as vascular density or vascular development. It has been shown that regional differences in neurovascular coupling do exist, measured as the relationship between $CMRO_2$ and CBF between the primary visual and primary motor cortex [Chiarelli et al., 2007], and are likely due to varied developmental and maturation patterns of these areas as well as their corresponding vascular architecture characteristics. For example, previous studies [Zuo et al., 2010b] show that the occipital lobe has a higher inflection age of homotopic connectivity than the other anatomical lobes. Also, it was shown that the heteromodal areas have the lowest inflection age, while unimodal is higher, and primary somato-motor is even higher. Language processing, a well-documented lateralized function, has also been shown to have increased CBF velocity in adolescents versus children in the left, but not the right hemisphere, showing the development of vasculature (i.e., vessel density) in agreement with regional functional differences [Haag et al., 2010]. In an attempt to better understand the involvement of structural and vascular development in the measured BOLD signal, advanced optical imaging

techniques can be used to characterize the underlying development and organization of the brain [Wu et al., 2013]. Also of interest is the behavior of the limbic system in response to hypercapnia, as there is no significant difference between NC1 and HC, but there is between HC and NC2. This may be due to the fact that most brain structures in the limbic system are heterotopic and have relatively low VMHC values [Zuo et al., 2010b]. In addition, the definition of limbic regions in the hierarchical and functional classifications is not consistent. Therefore, these relatively inconsistent HC results of the limbic system should be studied more carefully in the future using a more robust and well-defined network template.

Our findings may have important implications in interpreting RS-fMRI data. Fluctuations in arterial blood CO_2 can occur during normal breathing due to changes in breathing depth and rate, at a frequency of about 0.3 Hz of the respiratory signal. [Birn et al., 2006; Robbins et al., 1990; Wise et al., 2004]. These changes can influence CBF, and thus the amount of oxygen available to the tissue, which may in turn change the amount of BOLD response, as 8–9% of the BOLD signal's fluctuations can be attributed to CO_2 level changes [Wise et al., 2004]. Our findings may also help to identify the need and importance to correct physiological noise in patients with comorbid respiratory diseases that can lead to increased arterial CO_2 level. For proper analysis, the effects of the arterial CO_2 levels on the BOLD signal must be properly separated from the basic neural signal fluctuations. This separation, however, merits more research. Previous studies [Lund et al., 2006; Van Dijk et al., 2010; Windischberger et al., 2002] have investigated how to remove physiological variation from the BOLD signal. One method often used is to regress out the average signal within the ventricles and the white matter, as these regions contain relatively high proportion of noise caused by the cardiac and respiratory cycles. Another approach has been global signal regression at every voxel, as it is assumed that physiological noise will cause the same pattern of activation across all voxels in the brain [Macey et al., 2004]. However, this method of correction is still under debate [Hyder and Rothman, 2010].

To further test the hypercapnia influence and its remaining effect, we also performed the second room-air breathing scan shortly after the hyperpercapnia scan (waiting about 2 min to allow $EtCO_2$ to return to baseline). We found that changes in VMHC due to the hypercapnia challenge recovered prior to this normocapnic follow up scan, indicating that the decreased in synchronized activity is transient and directly dependent on arterial CO_2 levels. By showing the transient property of increased arterial CO_2 levels, the effects on the fMRI BOLD signal can be removed based on recorded physiological parameters without lingering effects, as the BOLD signal fluctuations follow $EtCO_2$ fluctuations on a second to second timeframe. Although the breath-by-breath effects of varying arterial CO_2 levels were not tested in the current study, these short term vascular effects are also evident in studies where cerebrovascular reactivity is measured by analyzing the changes in the BOLD signal amplitude in response to variation in the arterial CO_2 concentration levels [Yezhuvath et al., 2009]. Our study describes effects of increased arterial CO_2 in a highly controlled breathing paradigm, which suggests that naturally occurring level variations may be corrected.

Limitations of this study include the lack of CBF data. This additional data would help identify changes in the left and right vasculature of these subjects, and would help explain the differential regional effects of hypercapnia. However, this is outside of the scope of the current study and a thorough investigation of blood flow changes in response to increased arterial CO_2, would be a very useful study in the future, to assist functional MRI analysis methodology.

REFERENCES

Aaslid R (1987): Visually evoked dynamic blood flow response of the human cerebral circulation. Stroke 18:771–775.

Benson RR, FitzGerald DB, LeSueur LL, Kennedy DN, Kwong KK, Buchbinder BR, Davis TL, Weisskoff RM, Talavage TM, Logan WJ, Cosgrove GR, Belliveau JW, Rosen BR (1999): Language dominance determined by whole brain functional MRI in patients with brain lesions. Neurology 52:798–809.

Birn RM, Diamond JB, Smith MA, Bandettini PA (2006): Separating respiratory-variation-related fluctuations from neuronal-activity-related fluctuations in fMRI. NeuroImage 31:1536–1548.

Biswal B, Hudetz AG, Yetkin FZ, Haughton VM, Hyde JS (1997): Hypercapnia reversibly suppresses low-frequency fluctuations in the human motor cortex during rest using echo-planar MRI. J Cereb Blood Flow Metab 17:301–308.

Biswal BB, Kannurpatti SS, Rypma B (2007): Hemodynamic scaling of fMRI-BOLD signal: Validation of low-frequency spectral amplitude as a scalability factor. Magn Reson Imaging 25: 1358–1369.

Bulla-Hellwig M, Vollmer J, Gotzen A, Skreczek W, Hartje W (1996): Hemispheric asymmetry of arterial blood flow velocity changes during verbal and visuospatial tasks. Neuropsychologia 34:987–991.

Chen JJ, Pike GB (2010): Global cerebral oxidative metabolism during hypercapnia and hypocapnia in humans: Implications for BOLD fMRI. J Cereb Blood Flow Metab 30:1094–1099.

Chiarelli PA, Bulte DP, Gallichan D, Piechnik SK, Wise R, Jezzard P (2007): Flow-metabolism coupling in human visual, motor, and supplementary motor areas assessed by magnetic resonance imaging. Magn Reson Med 57:538–547.

Fair DA, Dosenbach NU, Church JA, Cohen AL, Brahmbhatt S, Miezin FM, Barch DM, Raichle ME, Petersen SE, Schlaggar BL (2007): Development of distinct control networks through segregation and integration. Proc Natl Acad Sci USA 104:13507–13512.

Friston KJ, Williams S, Howard R, Frackowiak RS, Turner R (1996): Movement-related effects in fMRI time-series. Magn Reson Med 35:346–355.

Gee DG, Biswal BB, Kelly C, Stark DE, Margulies DS, Shehzad Z, Uddin LQ, Klein DF, Banich MT, Castellanos FX, Milham MP (2011): Low frequency fluctuations reveal integrated and segregated processing among the cerebral hemispheres. NeuroImage 54:517–527.

Gur RC, Gur RE, Obrist WD, Hungerbuhler JP, Younkin D, Rosen AD, Skolnick BE, Reivich M (1982): Sex and handedness differences in cerebral blood flow during rest and cognitive activity. Science 217:659–661.

Haag A, Moeller N, Knake S, Hermsen A, Oertel WH, Rosenow F, Hamer HM (2010): Language lateralization in children using functional transcranial Doppler sonography. Dev Med Child Neurol 52:331–336.

Hyder F, Rothman DL (2010): Neuronal correlate of BOLD signal fluctuations at rest: Err on the side of the baseline. Proc Natl Acad Sci USA 107:10773–10774.

Ibler MJ, Lage S, Beck AM (1992): [Capnometry]. Ugeskrift for Laeger. 154:1161–1165.

Jain V, Langham MC, Floyd TF, Jain G, Magland JF, Wehrli FW (2011): Rapid magnetic resonance measurement of global cerebral metabolic rate of oxygen consumption in humans during rest and hypercapnia. J Cereb Blood Flow Metab 31:1504–1512.

Jones-Gotman M (1986): Memory for designs: The hippocampal contribution. Neuropsychologia 24:193–203.

Kelly C, Zuo XN, Gotimer K, Cox CL, Lynch L, Brock D, Imperati D, Garavan H, Rotrosen J, Castellanos FX, Milham MP (2011): Reduced interhemispheric resting state functional connectivity in cocaine addiction. Biol Psychiatry 69:684–692.

Kety SS, Schmidt CF (1948): The effects of altered arterial tensions of carbon dioxide and oxygen on cerebral blood flow and cerebral oxygen consumption of normal young men. J Clin Invest 27:484–492.

Kim SG, Rostrup E, Larsson HB, Ogawa S, Paulson OB (1999): Determination of relative CMRO2 from CBF and BOLD changes: Significant increase of oxygen consumption rate during visual stimulation. Magn Reson Med 41:1152–1161.

Kimura D, Archibald Y (1974): Motor functions of the left hemisphere. Brain 97:337–350.

Lu H, Xu F, Rodrigue KM, Kennedy KM, Cheng Y, Flicker B, Hebrank AC, Uh J, Park DC (2011): Alterations in cerebral metabolic rate and blood supply across the adult lifespan. Cereb Cortex 21:1426–1434.

Lu H, Liu P, Yezhuvath U, Cheng Y, Marshall O, Ge Y (2014): MRI mapping of cerebrovascular reactivity via gas inhalation challenges. J Vis Exp (94), e52306.

Lund TE, Madsen KH, Sidaros K, Luo WL, Nichols TE (2006): Non-white noise in fMRI: Does modelling have an impact? NeuroImage 29:54–66.

Macey PM, Macey KE, Kumar R, Harper RM (2004): A method for removal of global effects from fMRI time series. NeuroImage 22:360–366.

Mark CI, Fisher JA, Pike GB (2011): Improved fMRI calibration: Precisely controlled hyperoxic versus hypercapnic stimuli. NeuroImage 54:1102–1111.

Mark CI, Mazerolle EL, Chen JJ (2015): Metabolic and vascular origins of the BOLD effect: Implications for imaging pathology and resting-state brain function. J Magn Reson Imaging. doi: 10.1002/jmri.2478

Marshall O, Lu H, Brisset JC, Xu F, Liu P, Herbert J, Grossman RI, Ge Y (2014): Impaired cerebrovascular reactivity in multiple sclerosis. JAMA Neurol 71:1275–1281. doi: 10.1001/jamaneurol.2014.1668.

Mesulam MM (1998): From sensation to cognition. Brain 121:1013–1052.

Rihs F, Gutbrod K, Gutbrod B, Steiger HJ, Sturzenegger M, Mattle HP (1995): Determination of cognitive hemispheric dominance by "stereo" transcranial Doppler sonography. Stroke 26:70–73.

Robbins PA, Conway J, Cunningham DA, Khamnei S, Paterson DJ (1990): A comparison of indirect methods for continuous estimation of arterial PCO2 in men. J Appl Physiol (1985) 68:1727–1731.

Schmidt P, Krings T, Willmes K, Roessler F, Reul J, Thron A (1999): Determination of cognitive hemispheric lateralization by "functional" transcranial Doppler cross-validated by functional MRI. Stroke 30:939–945.

Schroeder CE, Lakatos P (2009): Low-frequency neuronal oscillations as instruments of sensory selection. Trends Neurosci 32:9–18.

Sicard KM, Duong TQ (2005): Effects of hypoxia, hyperoxia, and hypercapnia on baseline and stimulus-evoked BOLD, CBF, and CMRO2 in spontaneously breathing animals. NeuroImage 25: 850–858.

Stark DE, Margulies DS, Shehzad ZE, Reiss P, Kelly AM, Uddin LQ, Gee DG, Roy AK, Banich MT, Castellanos FX, Milham MP (2008): Regional variation in interhemispheric coordination of intrinsic hemodynamic fluctuations. J Neurosci 28:13754–13764.

Van Dijk KR, Hedden T, Venkataraman A, Evans KC, Lazar SW, Buckner RL (2010): Intrinsic functional connectivity as a tool for human connectomics: Theory, properties, and optimization. J Neurophysiol 103:297–321.

Windischberger C, Langenberger H, Sycha T, Tschernko EM, Fuchsjager-Mayerl G, Schmetterer L, Moser E (2002): On the origin of respiratory artifacts in BOLD-EPI of the human brain. Magn Reson Imaging 20:575–582.

Wise RG, Ide K, Poulin MJ, Tracey I (2004): Resting fluctuations in arterial carbon dioxide induce significant low frequency variations in BOLD signal. NeuroImage 21:1652–1664.

Wu Y, Christensen R, Colon-Ramos D, Shroff H (2013): Advanced optical imaging techniques for neurodevelopment. Curr Opin Neurobiol 23:1090–1097.

Xu F, Uh J, Brier MR, Hart J Jr, Yezhuvath US, Gu H, Yang Y, Lu H (2011): The influence of carbon dioxide on brain activity and metabolism in conscious humans. J Cereb Blood Flow Metab 31:58–67.

Yablonskiy DA (2011): Cerebral metabolic rate in hypercapnia: Controversy continues. J Cereb Blood Flow Metab 31:1502–1503.

Yeo BT, Krienen FM, Sepulcre J, Sabuncu MR, Lashkari D, Hollinshead M, Roffman JL, Smoller JW, Zollei L, Polimeni JR, Fischl B, Liu H, Buckner RL (2011): The organization of the human cerebral cortex estimated by intrinsic functional connectivity. J Neurophysiol 106:1125–1165.

Yezhuvath US, Lewis-Amezcua K, Varghese R, Xiao G, Lu H (2009): On the assessment of cerebrovascular reactivity using hypercapnia BOLD MRI. NMR Biomed 22:779–786.

Yuan R, Di X, Kim EH, Barik S, Rypma B, Biswal BB (2013): Regional homogeneity of resting-state fMRI contributes to both neurovascular and task activation variations. Magn Reson Imaging 31:1492–1500.

Zappe AC, Uludag K, Oeltermann A, Ugurbil K, Logothetis NK (2008): The influence of moderate hypercapnia on neural activity in the anesthetized nonhuman primate. Cereb Cortex 18: 2666–2673.

Zhou Y, Milham M, Zuo XN, Kelly C, Jaggi H, Herbert J, Grossman RI, Ge Y (2013): Functional homotopic changes in

multiple sclerosis with resting-state functional MR imaging. AJNR Am J Neuroradiol 34:1180–1187.

Ziyeh S, Rick J, Reinhard M, Hetzel A, Mader I, Speck O (2005): Blood oxygen level-dependent MRI of cerebral CO2 reactivity in severe carotid stenosis and occlusion. Stroke 36:751–756.

Zou QH, Zhu CZ, Yang Y, Zuo XN, Long XY, Cao QJ, Wang YF, Zang YF (2008): An improved approach to detection of amplitude of low-frequency fluctuation (ALFF) for resting-state fMRI: Fractional ALFF. J Neurosci Methods 172:137–141.

Zuo XN, Di Martino A, Kelly C, Shehzad ZE, Gee DG, Klein DF, Castellanos FX, Biswal BB, Milham MP (2010a): The oscillating brain: Complex and reliable. NeuroImage 49:1432–1445.

Zuo XN, Kelly CA, Martino D, Mennes M, Margulies DS, Bangaru S, Grzadzinski R, Evans AC, Zang YF Castellanos FX, Milham MP, (2010b): Growing together and growing apart: Regional and sex differences in the lifespan developmental trajectories of functional homotopy. J Neurosci 30:15034–15043.